Efficient Site-specific Low-energy Electron Production via Interatomic Coulombic Decay Following Resonant Auger Decay

M. Kimura,[1] H. Fukuzawa,[1] K. Sakai,[1] S. Mondal,[1] E. Kukk,[2]
Y. Kono,[3] S. Nagaoka,[3] Y. Tamenori,[4] N. Saito,[5] and K. Ueda[1,*]

[1]*Institute of Multidisciplinary Research for Advanced Materials, Tohoku University, Sendai 980-8577, Japan*
[2]*Department of Physics, University of Turku, FI-20014 Turku, Finland*
[3]*Department of Chemistry, Ehime University, Matsuyama 790-8577, Japan*
[4]*Japan Synchrotron Radiation Research Institute, Sayo, Hyogo 679-5198, Japan*
[5]*National Institute of Advanced Industrial Science and Technology, NMIJ, Tsukuba 305-8568, Japan*

(Dated: March 27, 2013)

We identified interatomic Coulombic decay (ICD) channels in argon dimers after spectator-type resonant Auger decay $2p^{-1}\ 3d \rightarrow 3p^{-2}3d, 4d$ in one of the atoms, using momentum resolved electron-ion-ion coincidence. The results illustrate that the resonant core excitation is a very efficient way of producing slow electrons at a specific site, which may cause localized radiation damage. We find also that ICD rate for $3p^{-2}4d$ is significantly lower than that for $3p^{-2}3d$.

PACS numbers: 36.40.Mr,33.80.Eh, 33.70.+e, 79.60.Jv,82.33.Fg

Though inner-valence vacancy states in molecules are usually not subject to autoionization, such states may be subject to autoionization if the inner-valence ionized molecule is close to other molecules. This new type of autoionization was noted by Cederbaum *et al.* [1] and called intermolecular or interatomic Coulombic decay (ICD). Since then, many theoretical and experimental studies have been reported in many different systems. See, e.g., recent review articles [2, 3]. It is now well-known that ICD appears everywhere and transfers the energy and the charge from the excited species to the environment surrounding it. Also it is known that there are many variants of ICD, such as ICD from satellite states [4–7], ICD after Auger decay [8–14], resonant ICD [15–17] where inner-valence excited states decay via ICD-like spectator decay, and 3-electron ICD [18, 19] where two inner-valence holes in a species are filled by ICD in which three electrons are involved. Another exotic variant, called electron-transfer-mediated decay (ETMD), was also predicted [20] and observed [21, 22].

Relevance of ICD processes with radiation damage is also noted [9, 23–27]. Noting that ICD produces low energy electrons locally at the site where an excitation takes place, one mayaW think one step further: one may consider the relevance of the production of low energy electron via ICD with radiation therapy that requires the localized radiation damage. Up to now, however, ICD has been studied with ionizing radiation that does not have a selectivity of the site or the states. Namely, in order to observe ICD, one usually ionizes the inner-valence orbital or populate the satellite state by the monochromatic radiation [4, 23, 24]. This radiation, however, not only populates the ICD initial state of the target atom or molecule at a specific site but also ionizes inner- and outer-valence orbitals of any atoms and molecules. Using core ionization by the radiation with photon energy above a core ionization potential of the specific atom may improve, to a certain amount, the selectivity of the atomic photoabsorption. ICD takes place from the Auger final states that have the inner-valence hole [8]. The branching ratio to these states are, however, only of the order of 10 % [9, 13, 19]. In turn, a well-established method of site-specific excitation is resonant core excitation; using the chemical shift, one can select not only a specific kind of atoms but also a specific site of the same kind of atoms located at different sites. Very recently, Gokhberg *et al.* suggested this pathway: the merits of this ICD mode are the high site-selectivity and the tunability of the ICD-electron energy using different resonant core excitations [28].

In the present work, we demonstrate that ICD indeed takes place following resonant Auger decay efficiently, with a probability close to 100 %. As a prototype sample, we have used argon dimers. The schematic sequence we have investigated is illustrated in Fig. 1. When a $2p$ electron in one of the atoms is excited to a $3d$ orbital, a spectator Auger decay takes place in the atom, populating mostly the spectator Auger final state $3p^{-2}3d$ and its shakeup state $3p^{-2}4d$ [Fig. 1(a)]. Then ICD takes place [Fig. 1(b)] from these states, leading to fragmentation to $Ar^+(3p^{-1})$-$Ar^+(3p^{-1})$ [Fig. 1(c)]. In the experiment, we record 3D momentum for each of two Ar^+ ions and the ICD electron in coincidence.

The experiment was carried out on the c branch of the beam line 27SU [29–31] at SPring-8. The storage ring was operated in several-bunches mode providing 53 single bunches (4/58 filling bunches) separated by 82.6 ns. The monochromatic radiation was directed horizontally, with vertical linear polarization. The argon dimers Ar_2 were produced by expanding argon gas at a stagnation pressure of 0.3 MPa at room temperature through a pinhole of 30 μm diameter. Under these conditions the cluster beam contains monomers, dimers, and a very small fraction of larger clusters. The

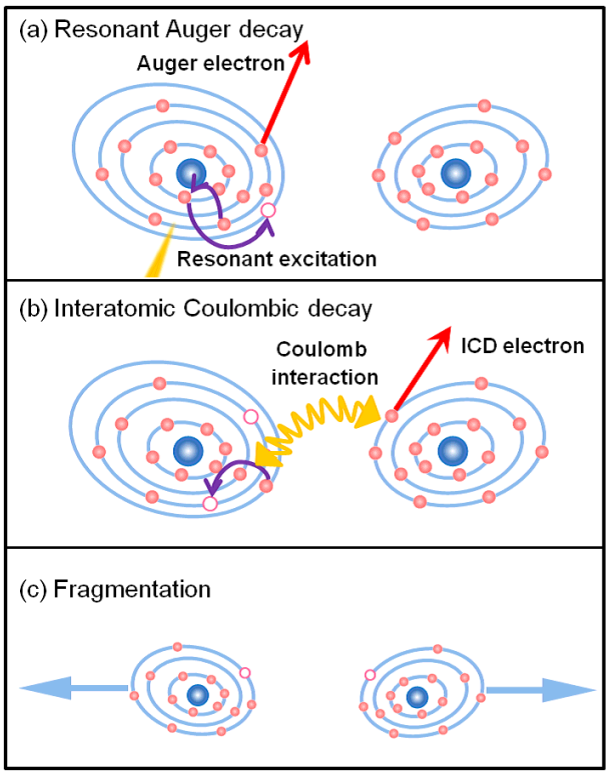

FIG. 1: (Color on line.) Sequence of events observed in the Ar dimer. (a) Photoexcitation promotes a $2p$ electron to an unoccupied $3d$ orbital in one of the atoms. The $2p$ vacancy is filled by one of the $3p$ electrons and another $3p$ electron is emitted from the same atom, while the $3d$ electron remains as a spectator (resonant Auger decay). (b) Interatomic Coulombic decay takes place, in which one of the two $3p$ vacancies is filled by the $3d$ electron from the same atom and the excess energy is transferred to the neighboring atom which in turn emits one of its $3p$ electrons. (c) Fragmentation due to Coulomb explosion takes place. The $Ar^+(3p^{-1})$ and $Ar^+(3p^{-1})$ fragment ions along with the ICD electron emitted in (b) are detected in coincidence.

signals from dimers were selected by applying the momentum conservation law for the ion pairs detected in coincidence (see below). The cluster beam was directed vertically and crossed the incident radiation at right angles. The incident energy was tuned to the excitation energy $2p_{3/2} \rightarrow 3d$ at 246.94 eV [32], with the photon band width of 0.13 eV.

Our momentum-resolved electron-ion multicoincidence [9, 33] is equivalent to cold-target recoil-ion momentum spectroscopy or reaction microscope [34] and is based on recording times of flight (TOFs) for electrons and ions with two position and time sensitive multihit-capable detectors (Roentdek HEX120 for electrons and HEX80 for ions). Knowledge of position and arrival time on the particle detectors, (x, y, t), allows us to extract information about the 3D momentum of each particle. The electron and ion spectrometers

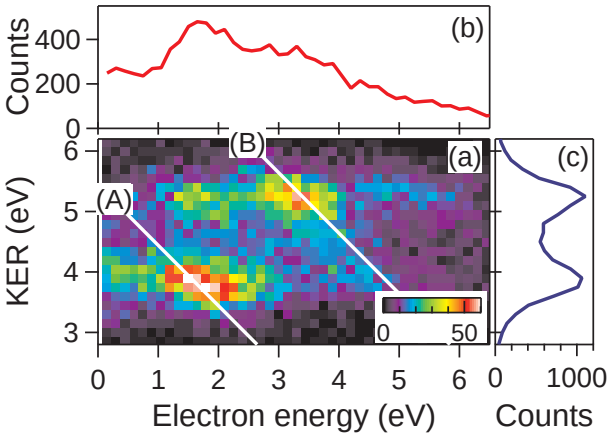

FIG. 2: (Color on line.) (a) Relationship between the electron energy and the total kinetic energy release (KER) of the Ar_2 fragmentation. (b) Electron energy distribution of the electron ejected from Ar dimers. (c) The KER of the Ar_2 fragmentation.

were placed face to face. The spectrometer axis was horizontal and perpendicular to both the incident radiation and the cluster beam. Electric and magnetic fields were applied to the interaction region, so that all the electrons with energy up to 22 eV and all the fragment ions were guided to the electron and ion detectors, respectively. Detailed geometric descriptions and typical field conditions of the spectrometers were given elsewhere [33]. The TOFs of electrons and ions were recorded with respect to the bunch marker of the light source using multi-hit time-to-digital converters (Roentdek TDC8HP), selecting by logic gating only electron signals synchronized with the single bunches.

The coincidence measurement for one electron and two ions provides the electron kinetic energy together with the kinetic energy release (KER) between the two Ar^+ ions for each event. The relationship of the electron energy and the KER is shown in Fig. 2(a). There are two prominent islands; one at electron energy of 1.8 eV and KER = 3.8 eV and the other at electron energy of 3.3 eV and KER = 5.2 eV. We may notice also that there is one more faint island at electron energy of 1.8 eV and KER = 5.2 eV. Figure 2(b) shows the electron energy distribution recorded in coincidence with the fragmentation into Ar^+-Ar^+. These electrons correspond to the ICD electrons, as we will discuss below. Figure 2(c) shows the distribution of the KER. There are two peaks, one at 3.8 eV and the other at 5.2 eV. If we assume the Coulomb repulsion between the two ions, then the corresponding internuclear distances are 3.8 Å and 2.8 Å, respectively. The bond-length of the neutral argon dimer is 3.76 Å [35]. Thus the peak at 3.8 eV corresponds to the case where ICD takes place at the equilibrium internuclear distance of the neutral

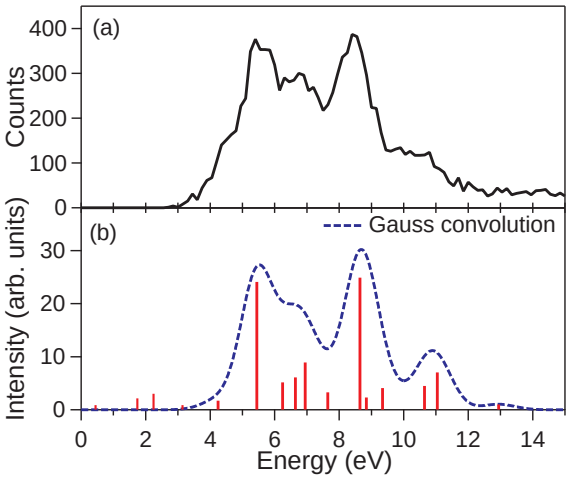

FIG. 3: (Color on line.) Energy distribution for the sum of the electron energy and the KER, as measured (a) and as estimated (b). The estimates given by the red bars in (b) are based on the resonant Auger transitions reported in [36]. See text and Table I for the details. The (blue) curve is a convolution of vertical lines by Gaussian profiles with 0.94 eV FWHM (i.e., the average experimental resolution) to compare with the experimental spectrum in (a). In the convolution the states below 4 eV given by thin red bars are excluded because the ICD channels are energetically closed.

TABLE I: Candidates of the ICD initial states, expected sum of electron kinetic energy and KER and relative intensities. The energies and the intensities are estimated from resonant Auger energies and intensities reported in [36]. The ICD channels are energetically closed for the states below 4 eV.

ICD initial state	Energy (eV)	Relative intensity
$3p^4(^3P)3d\ ^4D$	0.44	0.86
$^4F+^2P$	1.74	2.15
$^4P+^2F+^2D+4s^2D$	2.24	3.01
$(^1D)3d\ ^2G$	3.14	0.86
^2F	4.24	1.72
$^2D\ +\ ^2P$	5.44	24.08
$(^1S)3d\ ^2D$	6.24	5.16
$(^1D)3d\ ^2S$	6.64	5.16
$3p^4(^3P)4d\ ^4D$	6.64	0.94
$^4F+^4P+^2F$	6.94	8.93
$^2P+^2D$	7.64	3.29
$(^1D)4d\ ^2G+^2P+^2D+^2F$	8.64	24.91
^2S	9.34	1.88
$(^1S)4d\ ^2D$	11.04	7.05
$3p^4\ (^3P)5d\ ^4D+^4F+^4P+^2F$	8.84	2.30
$^2D+^2P$	9.34	2.20
$(^1D)5d\ ^2G+^2D+^2F+^2P+^2S$	10.64	4.50
$(^1S)5d\ ^2D$	12.94	1.00

argon dimer. The peak at 5.2 eV, on the other hand, corresponds to the case where ICD takes place at the internuclear distance significantly shorter (by $\sim$ 1 Å) than the equilibrium bond length.

The initial states of ICD are the final states of the resonant Auger decay following the $2p_{3/2} \rightarrow 3d$ excitation in one of the argon atoms (see Fig. 1). These resonant Auger final states are well known (see, for example [36]). The candidates of the ICD initial states are summarized in Table I. Some of these ICD initial states are the satellite states from which ICD transitions were observed [5]. The final states of the ICD are the lowest dicationic states of Ar_2 that dissociate to $Ar^+(3p^{-1}\ ^2P_{1/2,3/2})$ and $Ar^+(3p^{-1}\ ^2P_{1/2,3/2})$, whose weighted average energy is 31.64 eV relative to the two neutral atoms in the ground state. The energy difference between the energies of the ICD initial state and the sum energy of the two ionic fragments $Ar^+(3p^{-1}\ ^2P_{1/2,3/2})$ (i.e., 31.64 eV) are given in Table I. This amount of energy is shared among the ICD electron and two fragment ions. The distribution for the energy sum of the electron kinetic energy and the KER is illustrated in Fig. 3(a). From the resonant Auger final states given in Table I, ICD and radiative decay may take place. The radiative decay is expected to be much slower than ICD. Assuming that the these resonant Auger final states decay via only ICD as long as ICD is energetically open, the intensities of the individual ICD transitions are expected to be proportional to the populations of the ICD initial states. The populations can be estimated by the intensity ratios of the resonant Auger transitions that can be found in literature [36] as given in Table I. The positions of the vertical lines in Fig. 3(b) correspond to the expected energy sums for the ICD transitions and their heights correspond to the relative intensities of the corresponding resonant Auger transitions (see Table I). The intensity distribution for the ICD transitions thus estimated agree well with the present observation, as seen in Fig. 3. This agreement confirms that the resonant Auger final states are subject to ICD as long as ICD is energetically open and that other competing processes such as radiative decay is much slower than ICD.

The peak at 5.4 eV is assigned to the transition $Ar^+(3p^{-2}(^1D)3d\ ^2D)$-Ar $\rightarrow$ $Ar^+(3p^{-1})$-$Ar^+(3p^{-1})$, whereas the peak at 8.6 eV is assigned to the transition $Ar^+(3p^{-2}(^1D)4d\ ^2D)$-Ar $\rightarrow$ $Ar^+(3p^{-1})$-$Ar^+(3p^{-1})$. In Fig. 2(a), these two ICD transitions are indicated by the straight lines A and B of slope -1 with constant values of 5.4 and 8.6 eV for the sum of electron kinetic energy and KER. As noted above, the ICD transition $Ar^+(3p^{-2}(^1D)3d\ ^2D)$-Ar $\rightarrow$ $Ar^+(3p^{-1})$-$Ar^+(3p^{-1})$ [A in Fig. 2(a)] takes place at the equilib-

rium internuclear distance ~ 3.8 Å of the neutral argon dimer. This suggests that both the resonant Auger decay and the ICD are much faster than the vibrational motion of the argon dimer. On the other hand, the ICD transition $Ar^+(3p^{-2}(^1D)4d\ ^2D)$-Ar $\rightarrow$ $Ar^+(3p^{-1})$-$Ar^+(3p^{-1})$ [B in Fig. 2(a)] takes place at the internuclear distance ~ 2.8 Å that is significantly shorter than the equilibrium distance. This clearly illustrates that the ICD from $Ar^+(3p^{-2}(^1D)4d\ ^2D)$-Ar is significantly slower than that from $Ar^+(3p^{-2}(^1D)3d\ ^2D)$-Ar and takes place after bond-shrinking. It is worth noting that the ICD transition from $Ar^+(3p^{-2}(^1D)4d\ ^2D)$-Ar does not occur at nuclear distances smaller than $\sim$ 2.8 Å, though ICD is in principle energetically allowed there. Therefore, the internuclear distance 2.8 Å may correspond to the inner turning point of the classical vibrational motion for $Ar^+(3p^{-2}(^1D)4d\ ^2D)$-Ar. A recent theoretical study estimated that the turning point is ~ 2.6 Å [40], supporting our hypothesis. The ICD rate increases rapidly with the decrease in the nuclear distance. Thus, if the ICD is slower than the nuclear motion, ICD takes place mostly at this inner turning point where the ICD rate takes the maximum. A classical vibrational period of the argon dimer in the ground state is ~ 1 ps. Those of ICD initial states may be shorter. The travel time for the vibrational wavepacket to reach the inner turning point is therefore ~ 0.5 ps at most. Thus, the lifetime of $Ar^+(3p^{-2}(^1D)4d\ ^2D)$-Ar is expected to be longer than 0.5 ps while that of $Ar^+(3p^{-2}(^1D)3d\ ^2D)$-Ar should be much shorter than 0.5 ps. These different lifetimes were confirmed by the recent theoretical study that estimated the lifetimes $14 - 46$ fs for $Ar^+(3p^{-2}(^1D)3d\ ^2D)$-Ar and $0.5 - 1.4$ ps for $Ar^+(3p^{-2}(^1D)4d\ ^2D)$-Ar [40].

Relevance of ICD and radiation damage was noted several times in literature [9, 23–27] due to the following reason. Genotoxic damage by high-energy ionizing radiation, including the breaking of DNA strands in living cells, is not caused by direct ionization but is induced by the secondary electrons produced by the primary ionizing radiation. Boudaïffa *et al.* [38] found that low-energy (1 to 20 eV) electrons can break DNA strands. Hanel *et al.* [39] demonstrated that the uracil molecule, one of the base units of RNA, is efficiently fragmented by electrons with energies ≤ 1 eV, i.e., below the threshold for electronic excitations. The ICD induced by high-energy ionizing radiation may undergo in biological molecules in the biological environment. Kinetic energy of the ICD electron is much lower than that of the first-step Auger electron. Thus the low-energy ICD electrons may cause radiation damage. In turn, radiation therapy requires the radiation damage at a specific site. Core excitation with a monochromatic radiation may be specific to the site and thus the ICD following the resonant Auger decay produces the low-energy electron that may cause damage to a specific site.

In conclusion, we demonstrated that the most of the resonant Auger final states decay via ICD, using Ar_2 as a prototype sample and tuning the excitation photon energy to the $2p \rightarrow 3d$ resonance. Since the resonant core excitation is intrinsically site specific, the present study implicates a new way to produce low energy electrons at high efficiency, causing local radiation damage at a specific site. We found also that the lifetime of $Ar^+(3p^{-2}(^1D)4d\ ^2D)$-Ar is longer than the lifetime of the $Ar^+(3p^{-2}(^1D)3d\ ^2D)$-Ar.

We are grateful to K. Gokhberg, A.I. Kuleff, P. Demekhin, and L.S. Cederbaum for stimulating discussion, K. Gokhberg for providing us with theoretical results prior to publication, U. Hergenhahn for critical reading the manuscript, and to K. Nagaya and M. Yao for their instruction of the sample beam preparation. The experiments were performed at SPring-8 with the approval of JASRI. The work was supported by Grant-in-Aid (21244062) from JSPS and by the Management Expenses Grants for National Universities Corporations from MEXT.

Note added: The CID after resonant Auger decay in the N_2 and CO dimers has been very recently independently observed [41].

* ueda@tagen.tohoku.ac.jp

[1] L.S. Cederbaum, J. Zobeley, and F. Tarantelli, Phys. Rev. Lett. **79**, 4778 (1997).
[2] V. Averbukh *et al.*, J. Electr. Spectr. Relat. Phenom. **183**, 36 (2011).
[3] U. Hergenhahn, J. Electr. Spectr. Relat. Phenom **184**, 78 (2011).
[4] T. Jahnke *et al.*, Phys. Rev. Lett. **99**, 153401 (2007).
[5] P. Lablanquie *et al.*, J. Chem. Phys. **127**, 154323 (2007).
[6] T. Havermeier *et al.*, Phys. Rev. Lett. **104**, 133401 (2010).
[7] N. Sisourat *et al.*, Nature Physics **6**, 508 (2010).
[8] R. Santra and L.S. Cederbaum, Phys. Rev. Lett. **90**, 153401 (2003); **94**, 199901(E)(2005).
[9] Y. Morishita *et al.*, Phys. Rev. Lett. **96**, 243402 (2006).
[10] Y. Morishita *et al.*, J. Phys. B: At. Mol. Opt. Phys. **41**, 025101 (2008).
[11] K. Kreidi *et al.*, J. Phys. B: At. Mol. Opt. Phys. **41**, 101002 (2008).
[12] M. Yamazaki *et al.*, Phys. Rev. Lett. **101**, 043004 (2008).
[13] K. Kreidi *et al.*, Phys. Rev. A **78**, 043422 (2008).
[14] K. Kreidi *et al.*, Phys. Rev. Lett. **103**, 033001 (2009).
[15] S. Barth *et al.*, J. Chem. Phys. **122**, 241102 (2011).
[16] T. Aoto *et al.*, Phys. Rev. Lett. **97**, 243401 (2006).
[17] K. Gokhberg, V. Averbukh, and L.C. Dederbaum, J. Chem. Phys. **124**, 144305 (2006).
[18] V. Averbukh and P. Kolorenc, Phys. Rev. Lett. **103**, 183001 (2009).
[19] T. Ouchi *et al.*, Phys. Rev. Lett. **107**, 053401 (2011).

[20] J. Zobeley, R. Santra, and L.S. Cederbaum, J. Chem. Phys. **115**, 5076 (2001).
[21] K. Sakai *et al.*, Phys. Rev. Lett. **106**, 033401 (2011).
[22] M. Förstel, M. Mucke, T. Arion, A.M. Bradshaw, and U. Hergenhahn, Phys. Rev. Lett. **106**, 033402 (2011).
[23] T. Jahnke *et al.*, Nature Physics **6**, 139 (2010).
[24] M. Mucke *et al.*, Nature Physics **6**, 143 (2010).
[25] O. Vendrell, S. D. Stoychev, and L.S. Cederbaum, Chem. Phys. Chem. **11**, 1006 (2010).
[26] S.D. Stoychev, A.I. Kuleff, and L.S. Cederbaum, J. Am. Chem. Soc. **133**, 6817 (2011).
[27] H.-K. Kim *et al.*, Proc. Nat. Acad. Sci. **108**, 11821 (2011).
[28] K. Gokhberg, P. Kolorenc, A. I. Kuleff, and L. S. Cederbaum, submitted to Science.
[29] H. Ohashi *et al.*, Nucl. Instrum. Methods A **467-468**, 529 (2001).
[30] H. Ohashi *et al.*, Nucl. Instrum. Methods A **467-468**, 533 (2001).
[31] K. Ueda, J. Phys. B: At. Mol. Opt. Phys. **36**, R1 (2003).
[32] M. Kato *et al.*, J. Electr. Spectosc. Relat. Phenom. **160**, 39 (2007).
[33] K. Ueda *et al.*, J. Electr. Spectosc. Relat. Phenom. **166-167**, 3 (2008).
[34] J. Ullrich, R. Moshammer, A. Dorn, R. Dörner, L.Ph.H. Schmidt, H. Schmidt-Böcking, Rep. Prog. Phys. **66**, 1463 (2003).
[35] J.F. Ogilvie and F.Y.H. Wang, J. Mol. Struct. **273**, 277 (1992).
[36] M. Meyer, E. v. Ravan, B. Sonntag, and J. E. Hansen, Phys. Rev. A **43**, 177 (1991).
[37] U. Fano and J. Cooper, Rev. Mod. Phys. **40**, 441 (1968).
[38] B. Boudaïffa, P. Cloutier, D. Hunting, M. A. Huels, and L. Sanche, Science **287**, 1658 (2000).
[39] G. Hanel *et al.*, Phys. Rev. Lett., **90**, 188104 (2003).
[40] K. Gokhberg, private communication.
[41] F. Trinter, M.S. Schöffler, H.-K. Kim, F. Sturm K. Cole, N. Neumann, A. Vredenborg, J. Williams, I. Bocharova, R. Guillemin, M. Simon, A. Belkacem, A. L. Landers, Th. Weber, H.Schmidt-Böcking, R. Dörner, and T. Jahnke, submitted to Science.